Precise Measurement of the $e^+e^- \to D_s^+D_s^-$ Cross Section at Center-of-Mass Energies from Threshold to 4.95 GeV

M. Ablikim *et al.*[*]
(BESIII Collaboration)

(Received 24 March 2024; revised 6 November 2024; accepted 26 November 2024; published 26 December 2024)

Using the e^+e^- collision data collected with the BESIII detector operating at the BEPCII collider, at center-of-mass energies from the threshold to 4.95 GeV, we present precise measurements of the cross section for the process $e^+e^- \to D_s^+D_s^-$ using a single-tag method. The resulting cross section line shape exhibits several new structures, thereby offering an input for a future coupled-channel analysis and model tests, which are critical to understand vector charmonium-like states with masses between 4 and 5 GeV.

DOI: 10.1103/PhysRevLett.133.261902

Quantum chromodynamics (QCD) predicts the confinement phenomenon in the low-energy region where hadrons are formed. A detailed study of hadron systems is essential for a better understanding of the nonperturbative effect of QCD. An important milestone in hadron physics is the discovery of the vector charmonium-like states, such as the $\psi(4230)$ in the $e^+e^- \to \pi^+\pi^- J/\psi$ process [1,2], and the $\psi(4360)$ and $\psi(4660)$ in the $e^+e^- \to \pi^+\pi^-\psi(3686)$ process [3,4]. These states exhibit properties that do not match the expectations for pure $c\bar{c}$ states. Since the masses of these states lie above the open-charm threshold, measurement of their couplings to the open-charm channels is crucial for understanding their nature. However, such studies are very complicated due to the presence of coupled-channel effects. Utilizing a coupled-channel approach for a simultaneous fit of the data allows for the extraction of parameters of these states, which significantly aids in elucidating their nature. The knowledge of exclusive open-charm cross sections, such as the cross sections of $e^+e^- \to D_s^+D_s^-$, serves as valuable information for a future coupled-channel analysis [5].

Furthermore, new structures have been seen around $E_{\rm cm} = 4.7$ GeV in $e^+e^- \to K^+K^-J/\psi$ with a significance over 5σ [6], and in $K_S^0K_S^0J/\psi$ with 4.2σ [7], while the fit result for $e^+e^- \to D_s^{*+}D_s^{*-}$ suggests a new structure around $E_{\rm cm=}4.79$ GeV with a significance of 6σ [8]. The similarity in quark composition with final state particles make $e^+e^- \to D_s^+D_s^-$ a promising candidate process for further investigation of the observed structures.

Although the Belle and *BABAR* experiments have measured the exclusive cross section for $e^+e^- \to D_s^+D_s^-$ through initial-state radiation (ISR) processes [9,10], the precision is not sufficient to pin down the complex correlations between the $\psi(4230)$ and nonresonant $e^+e^- \to D_s^+D_s^-$ production, which may involve interference, coupling effects, and other dynamical or kinematical factors. The CLEO-c experiment studied the process $e^+e^- \to D_s^+D_s^-$ [11] using energy scan data, with the maximum center-of-mass energy ($E_{\rm cm}$) of only 4.26 GeV.

The BESIII detector [12,13] has collected larger data samples more densely over a broader energy range compared to CLEO-c, Belle, and *BABAR*. This allows for improved accuracy in measurements of the exclusive open-charm cross sections. One example is the recent publication of the $e^+e^- \to D_s^{*+}D_s^{*-}$ cross section, where an unusual cross section line shape is observed [8]. The cross section of $e^+e^- \to D_s^+D_s^-$ is measured in the $E_{\rm cm}$ range between 3.94 and 4.95 GeV with 138 energy points corresponding to an integrated luminosity of 22.9 fb^{-1} in total.

To optimize the event selection criteria, determine the detection efficiency, and estimate the backgrounds, we produce simulated samples using the GEANT4-based [14] Monte Carlo (MC) software, which includes the geometric description of the BESIII detector and its response. The beam energy spread and ISR are taken into account with the generator KKMC [15,16]. The signal MC samples of the $e^+e^- \to D_s^+D_s^-$ process are generated for each sample, where the vector state decays into two scalar particles using EvtGen [17,18], and the $D_s^+ \to K^+K^-\pi^+$ decay is generated with the Dalitz model [19,20]. Final-state radiation from charged particles is simulated with the PHOTOS package [21]. To estimate possible background contributions, we generate inclusive and exclusive MC samples modeled with EvtGen using branching fractions taken from the particle data group (PDG) [22] for the known decay modes, and with LUNDCHARM [23] for the remaining unknown

[*]Full author list given at the end of the Letter.

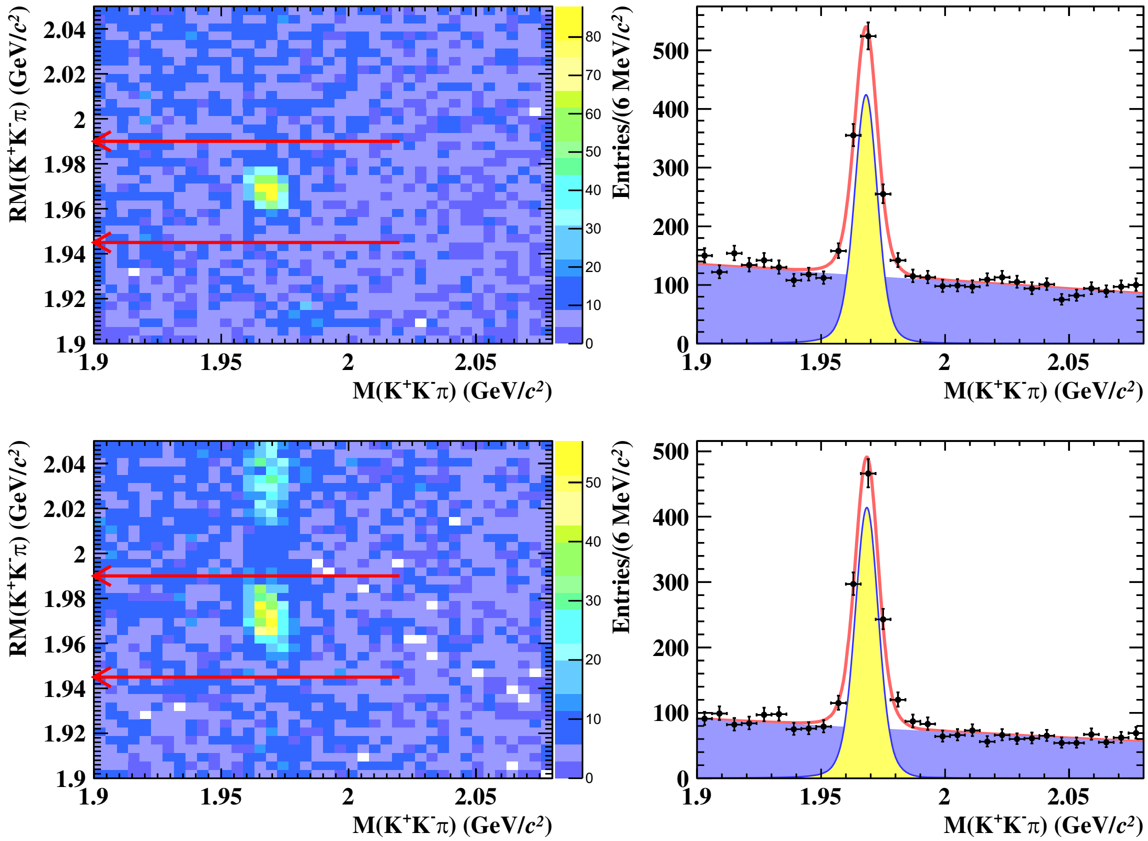

FIG. 1. The distribution plot of $RM(D_s^{\pm})$ versus $M(K^+K^-\pi^-)$ (left) and the fit to $M(K^+K^-\pi^-)$ (right) for data at $E_{\rm cm} = 4.26$ (first row) and 4.68 (second row) GeV. The signal interval is indicated by the red arrows. The fit to the $M(K^+K^-\pi)$ distribution is shown in the right panels as a red curve, with the background shape in blue and signal shape in yellow.

charmonium decays. Inclusive MC samples include all the possible processes in electron positron collisions. The integrated luminosities of the inclusive samples are comparable to those of data. For known processes, we generate the corresponding samples based on their cross sections. In the case of unknown processes, we assume they originate from a $J^{PC} = 1^{--}$ state, regardless of whether it corresponds to a charmonium state or is the result of nonresonant production via a virtual photon. The open-charm processes, light hadron processes, and quantum electrodynamic processes are used to check background components, and the result shows that no peaking background is found after our selection, except for the $e^+e^- \to D_s^* D_s$ process. Exclusive $e^+e^- \to D_s^* D_s$ MC samples, of which the luminosities are equivalent to ten times the data, are generated using helicity-amplitude (HELAMP) models at $E_{\rm cm} > 4.6$ GeV. The HELAMP inputs (relative magnitudes of the helicity amplitudes) are based on the $1 + \cos^2\theta$ distribution of helicity angle for both the $e^+e^- \to D_s^* D_s$ production and D_s^* decays.

Exploiting the low background level and high detection efficiency at BESIII, we only reconstruct the $D_s^- \to K^+K^-\pi^-$ decay, while D_s^+ is tagged by the recoil mass. The charge-conjugated modes are implied throughout this Letter, and the tagged D_s will always be referred to as D_s^-. Selection and identification of charged particles are performed using the same criteria as described in Ref. [24]. An event is labeled as a single-tag candidate if it contains at least one K^+K^- pair and at least one charged pion. All single-tag candidates are kept for further analysis. To improve the signal purity, we select the D_s^- candidates with two intermediate decay modes: $D_s^- \to \phi\pi^-$ with $\phi \to K^+K^-$ or $D_s^- \to K^*(892)^0 K^-$ with $K^*(892)^0 \to K^+\pi^-$. The $D_s^- \to \phi\pi^-$ decays are selected requiring the invariant mass of K^+K^- to satisfy $1.005 < M(K^+K^-) < 1.035$ GeV$/c^2$. To select the $D_s^- \to K^*(892)^0 K^-$ decays, we apply the requirements on the $K^+\pi^-$ invariant mass of $0.832 < M(K^+\pi^-) < 0.928$ GeV$/c^2$ and on the helicity angle of $|\cos\theta_{K^+ {\rm in} K^+\pi^-}| < 0.52$. The helicity angle is defined as the angle between the $K^*(892)^0$ and the D_s^- in the $K^*(892)^0$ rest frame.

Figure 1 (left) shows the scatter plot of the invariant mass of the selected $K^+K^-\pi$ combination [$M(K^+K^-\pi)$] versus its corrected recoil mass RM for data at $E_{\rm cm} = 4.26$ and 4.68 GeV. The $RM \equiv M^{\rm recoil}_{K^+K^-\pi^-} + M(K^+K^-\pi^-) - m(D_s^-)$ here is defined to improve the resolution of the recoil mass, where $M^{\rm recoil}_{K^+K^-\pi^-} \equiv |p_{e^+e^-} - p_{K^+} - p_{K^-} - p_{\pi^-}|$, $p_{e^+e^-}$, p_{K^+}, p_{K^-}, and p_{π^-} are the four momenta of the initial e^+e^-

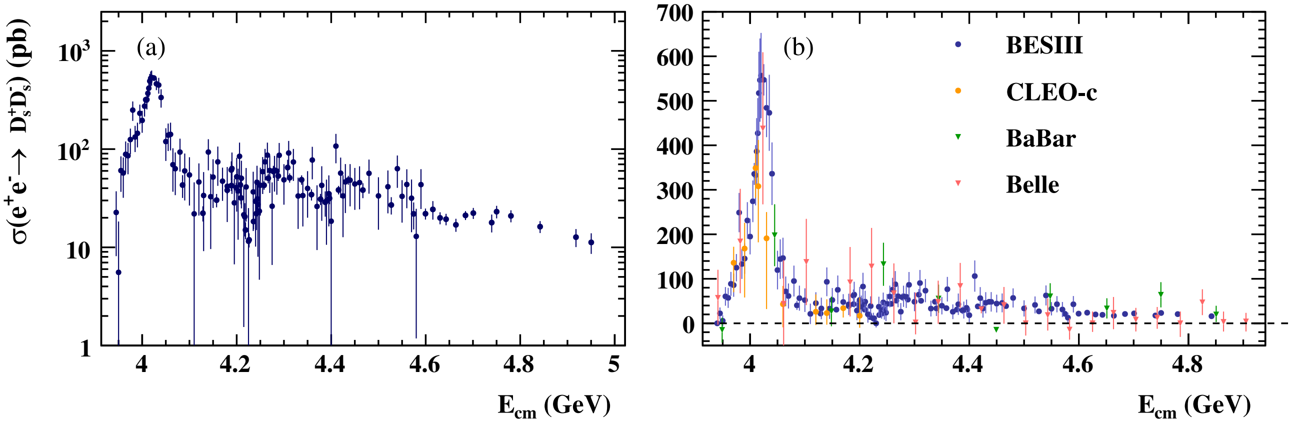

FIG. 2. The measured Born cross section of $e^+e^- \to D_s^+ D_s^-$ in logarithmic coordinates (a), where the error bars include the statistical and systematic uncertainties. The comparison between our measurements and those of *BABAR*, Belle, and CLEO-c (after ISR correction) (b).

system, the selected K^+, K^-, and π^-, respectively, and $m(D_s^-)$ is the nominal mass of D_s^- [22]. To suppress the background, the RM is required to be within the expected signal window, $1.945 < RM < 1.990\ \mathrm{GeV}/c^2$, as shown in Fig. 1 (left). The concentration of events at high RM is the tail of the $D_s D_s^*$ background, which peaks at $M(D_s^*)$.

In order to obtain the signal yields, we use the signal MC shape convolved with a Gaussian function as an alternative signal description to fit the $M(K^+K^-\pi)$ distribution after applying all the above requirements. The differences between MC simulation and data are taken into account with the mass shift Δm and the resolution $\Delta\sigma$ of the Gaussian function. At all energy points, $\Delta\sigma$ is fixed to the average value of 2.4 MeV to improve the fit stability for the low-statistics samples, while Δm is a free parameter of the fit at each energy point. The background is described with a linear function. The fits to $M(K^+K^-\pi)$ for data at $E_{\mathrm{cm}} = 4.26$ GeV and 4.68 GeV are shown in Fig. 1 (right) as examples.

Studies of the inclusive MC samples show that the $e^+e^- \to D_s^+ D_s^{*-}$ process contributes as a source of peaking background at $E_{\mathrm{cm}} > 4.6$ GeV. The estimated numbers of the D_s^+ signal events from $e^+e^- \to D_s^+ D_s^{*-}$ (defined as $N_{D_s^\pm D_s^{\mp *}}$) are obtained from exclusive MC samples normalized to the corresponding integrated luminosity and cross section, and are subtracted when calculating the number of signal events. The process $e^+e^- \to D_s^{*+} D_s^{*-}$ fails the recoil mass requirement, as its $RM(D_s^-)$ is concentrated above 2.1 GeV, making the signal contamination by this background negligible.

The Born cross section of $e^+e^- \to D_s^+ D_s^-$ is determined with

$$\sigma_{\mathrm{Born}} = \frac{N_{D_s}^{\mathrm{fit}} - N_{D_s^\pm D_s^{\mp *}}}{2\mathcal{B}(D_s^\pm \to K^+K^-\pi^\pm)\epsilon(1+\delta)\frac{1}{|1-\Pi|^2}\mathcal{L}}, \quad (1)$$

where $N_{D_s}^{\mathrm{fit}}$ is obtained from the fit to the $M(K^+K^-\pi^\pm)$ distribution in data. The factor $1/2$ takes into account the contributions from reconstruction of both $Ds+$ and $Ds-$. The parameter $N_{D_s^\pm D_s^{\mp *}}$ is the number of peaking background from $e^+e^- \to D_s^+ D_s^{*-}$, which is only present at $E_{\mathrm{cm}} > 4.6$ GeV. $\mathcal{L}$ is the integrated luminosity, $(1/|1-\Pi|^2)$ is the vacuum polarization [25] factor, and $\mathcal{B}(D_s^\pm \to K^+K^-\pi^\pm)$ is the branching fraction of $D_s^\pm \to K^+K^-\pi^\pm$, which is taken from Ref. [22]. $(1+\delta)$ is the ISR correction factor, and ϵ is the detection efficiency, using the interpolated values.

During the correction iterations, we use an MC-weighting method for radiative corrections and the efficiencies, in which the correction factors are evaluated iteratively. Initially, $(1+\delta)$ and ϵ are obtained by using KKMC simulation with a flat Born cross section line shape as input. Once the initial values are obtained, a smoothed line shape of cross section is derived using a variable span smoother [26,27]. By utilizing the smoothed cross section line shape, the MC-weighting method [28] is employed to update the efficiencies, ISR correction factors, and measured cross section. After five iterations, the Born cross sections converge to the values shown in Fig. 2, with detailed numbers provided in Supplemental Material [29].

Several features are observed in Fig. 2(a). First, the cross section peak above the $D_s^+ D_s^-$ threshold appears around $E_{\mathrm{cm}} = 4.02$ GeV, which is close to the mass of the known $\psi(4040)$. However, the width of this structure, estimated with a Breit–Wigner function fit, is about 40 ± 4 MeV, narrower than the 80 ± 10 MeV width of $\psi(4040)$ previously measured [22]. This narrower width implies the presence of a strong coupled-channel effect as predicted in Ref. [35].

The cross sections are generally consistent with previous experimental measurements, including those from Belle, *BABAR*, and CLEO-c after ISR correction [36], as shown in Fig. 2(b). To show more information about our results, the rough comparison is made without standardizing the experimental E_{cm} resolutions. Our measurements near 4.02 GeV show a maximum cross section larger than

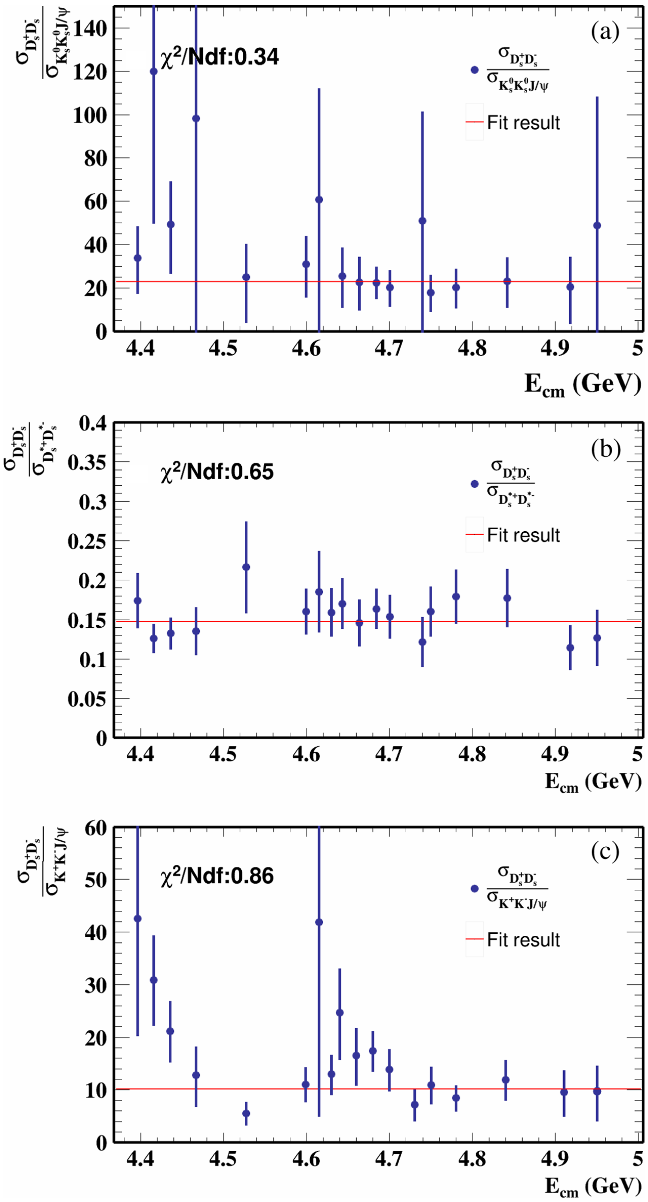

FIG. 3. The Born cross section ratios between $e^+e^- \to D_s^+D_s^-$ and $e^+e^- \to K_S^0K_S^0J/\psi$ (a). The Born cross section ratios between $e^+e^- \to D_s^+D_s^-$ and $e^+e^- \to D_s^{*+}D_s^{*-}$ (b). The Born cross section ratios between $e^+e^- \to D_s^+D_s^-$ and $e^+e^- \to K^+K^-J/\psi$ (c). Only statistical uncertainties are included.

500 pb, where not so many energy points are taken by the CLEO-c, *BABAR*, or Belle experiments.

The second notable feature is a narrow dip observed around $E_{\rm cm} = 4.23$ GeV, which is close to the $D_s^{*+}D_s^{*-}$ threshold (4.224 GeV) and the peak of the $\psi(4230)$. This phenomenon may reflect the influence of the open-channel effect of $e^+e^- \to D_s^{*+}D_s^{*-}$ on the cross section line shape of $e^+e^- \to D_s^+D_s^-$. It is important to note that the decay width of $\psi(4230) \to f_0(980)J/\psi$ [37,38] is not negligible, and the $f_0(980)$ particle contains a significant $s\bar{s}$ component [39]. Since the $s\bar{s}$ quark pair is also present in the $e^+e^- \to D_s^+D_s^-$ process, the observation of this dip offers valuable insights into the aforementioned nature of the $\psi(4230)$. If we disregard this dip, another notable observation is a potential broad structure spanning from $E_{\rm cm} = 4.1$ to 4.4 GeV.

Apart from those two prominent features, our measured line shape exhibits similarities in trends with the previously reported $e^+e^- \to D_s^{*+}D_s^{*-}$ [8], $e^+e^- \to K^+K^-J/\psi$ [6,40], and $e^+e^- \to K_S^0K_S^0J/\psi$ [7] processes above $E_{\rm cm} = 4.4$ GeV. The Born cross section ratios $[\sigma(e^+e^+ \to D_s^+D_s^-)/(e^+e^- \to K_S^0K_S^0J/\psi)]$, $[\sigma(e^+e^+ \to D_s^+D_s^-)/\sigma(e^+e^- \to D_s^{*+}D_s^{*-})]$, and $[\sigma(e^+e^+ \to D_s^+D_s^-)/\sigma(e^+e^- \to K^+K^-J/\psi)]$ are shown in Fig. 3. Fits to the ratios with constant values give $\chi^2/\mathrm{ndf} = 0.34$, 0.65, and 0.86, respectively, where ndf is the number of degrees of freedom.

The systematic uncertainty of the cross section measurement includes two groups of contributions: independent and common for all energy points.

The common systematic uncertainties include uncertainties related to the integrated luminosity, tracking, particle identification (PID), fit range, and cross section as shown in Table I. The integrated luminosities are measured with Bhabha and digamma events [41] with a systematic uncertainty of 1%. The PID is performed on two kaons and one pion, and the corresponding systematic uncertainty is 1% per track [42]. The uncertainty of tracking efficiency is estimated to be 1% per track [43]. Therefore, a 3% systematic uncertainty is assigned for both the tracking efficiency and PID. The uncertainty due to the fit range is estimated to be 2% by varying the mass range by 10 MeV. The systematic uncertainty on the $(D_s^{\pm}D_s^{*\mp})$ background contribution is negligible based on the uncertainties of cross section from the ongoing BESIII measurement.

TABLE I. Common relative systematic uncertainties in the measured Born cross section.

Source	$\sigma_{\rm sys}$ (%)
Tracking	3
Particle identification	3
$\mathcal{B}(D_s^{\pm} \to K^+K^-\pi^{\pm})$	1.9
Integrated luminosity	1
Fit range	2
Total	5.3

We only evaluate energy-dependent systematic uncertainties at 28 high-statistics energy points from the *XYZ* samples. The systematic uncertainties for the samples with low statistics are estimated using the values obtained from those nearby energy points with high statistics. We consider four sources of energy-dependent systematic uncertainties, including two mass windows and the choice of the signal and background shapes used in the fits. The uncertainties of the mass windows of ϕ and K^{*0} arise due to the difference in mass resolution between data and MC simulation. To evaluate the effect, the invariant mass distribution in the MC sample is smeared by a Gaussian distribution to obtain an agreement in mass resolution with the data. The relative change of the selection efficiency due to the smearing is taken as the systematic uncertainty. The uncertainty due to the signal shape is estimated by comparing fit results when the $\Delta(\sigma)$ parameter is fixed to 2.4 MeV and when it is used as a free parameter of the fit. The uncertainty due to the background shape is estimated by describing the background with a second-order polynomial instead of a linear function. The uncertainty due to the vacuum polarization is negligible [25]. The energy-dependent systematic uncertainties range from 1.1% to 4.2%, dominated by the contribution from the signal shape. Since ISR correction depends on the dressed cross section line shape, the difference of smoothed line shapes estimated with and without statistical uncertainties is considered as its systematic uncertainty. These are assigned to be 3% in the energy interval (4.215,4.235) GeV where the line shape changes most dramatically, 2% in (4.235,4.243) and (4.395,4.42) GeV, and 1% in all other energy intervals.

The total systematic uncertainties are calculated by summing all individual items in quadrature, which vary within (5.6–6.7)%. All the systematic uncertainties, including the individual contributions and the total ones, are presented as a covariance matrix in Supplemental Material [29].

In summary, we present precise measurements of the cross section for the process $e^+e^- \to D_s^+D_s^-$ for $E_{\rm cm}$ ranging from 3.94 to 4.95 GeV. Several notable features are observed in the cross section line shape. First, a significantly narrower width of the $\psi(4040)$ than the PDG value is observed. Second, a dip around the $D_s^{*+}D_s^{*-}$ threshold and the peak position of the $\psi(4230)$ is observed, suggesting the influence of the open-channel effect.

Instead of performing a fit to the cross section line shape using conventional Breit–Wigner functions, we provide the cross section values, their uncertainties, and a correlation matrix directly for further investigation. This is motivated by the challenges in accurately fitting the line shape when strong coupled-channel effects are present. These measurements open up a new avenue to test models explaining the nature of the $\psi(4230)$ and other vector charmonia and charmonium-like states [44] as well as perform coupled-channel fits involving multiple channels [45].

Acknowledgments—The BESIII Collaboration thanks the staff of BEPCII and the IHEP computing center for their strong support. This work is supported in part by National Key R&D Program of China under Contracts No. 2020YFA0406300, No. 2020YFA0406400, and No. 2023YFA1606000; National Natural Science Foundation of China (NSFC) under Contracts No. 11635010, No. 11735014, No. 11835012, No. 11935015, No. 11935016, No. 11935018, No. 11961141012, No. 12025502, 12035009, No. 12035013, No. 12061131003, No. 12192260, No. 12192261, No. 12192262, No. 12192263, No. 12192264, No. 12192265, No. 12221005, No. 12225509, No. 12235017, and No. 12150004; Program of Science and Technology Development Plan of Jilin Province of China under Contracts No. 20210508047RQ and No. 20230101021JC; the Chinese Academy of Sciences (CAS) Large-Scale Scientific Facility Program; the CAS Center for Excellence in Particle Physics (CCEPP); Joint Large-Scale Scientific Facility Funds of the NSFC and CAS under Contract No. U1832207; CAS Key Research Program of Frontier Sciences under Contracts No. QYZDJ-SSW-SLH003 and No. QYZDJ-SSW-SLH040; 100 Talents Program of CAS; the Institute of Nuclear and Particle Physics (INPAC) and Shanghai Key Laboratory for Particle Physics and Cosmology; European Union's Horizon 2020 research and innovation programme under Marie Sklodowska-Curie grant agreement under Contract No. 894790; German Research Foundation DFG under Contract No. 455635585, Collaborative Research Center CRC 1044, FOR5327, GRK 2149; Istituto Nazionale di Fisica Nucleare, Italy; Ministry of Development of Turkey under Contract No. DPT2006K-120470; National Research Foundation of Korea under Contract No. NRF-2022R1A2C1092335; National Science and Technology fund of Mongolia; National Science Research and Innovation Fund (NSRF) via the Program Management Unit for Human Resources & Institutional Development, Research and Innovation of Thailand under Contract No. B16F640076; Polish National Science Centre under Contract No. 2019/35/O/ST2/02907; the Swedish Research Council; and the U.S. Department of Energy under Contract No. DE-FG02-05ER41374.

[1] B. Aubert *et al.* (*BABAR* Collaboration), Phys. Rev. Lett. **95**, 142001 (2005).
[2] C. Z. Yuan *et al.* (Belle Collaboration), Phys. Rev. Lett. **99**, 182004 (2007).
[3] X. L. Wang *et al.* (Belle Collaboration), Phys. Rev. Lett. **99**, 142002 (2007).
[4] J. P. Lees *et al.* (*BABAR* Collaboration), Phys. Rev. D **89**, 111103(R) (2014).
[5] E. Eichten, K. Gottfried, T. Kinoshita, K. D. Lane, and T.-M. Yan, Phys. Rev. D **17**, 3090 (1978).
[6] M. Ablikim *et al.* (BESIII Collaboration), Phys. Rev. Lett. **131**, 211902 (2023).
[7] M. Ablikim *et al.* (BESIII Collaboration), Phys. Rev. D **107**, 092005 (2023).
[8] M. Ablikim *et al.* (BESIII Collaboration), Phys. Rev. Lett. **131**, 151903 (2023).
[9] G. Pakhlova *et al.* (Belle Collaboration), Phys. Rev. D **83**, 011101 (2011).

[10] P. del Amo Sanches *et al.* (*BABAR* Collaboration), Phys. Rev. D **82**, 052004 (2010).
[11] D. Cronin-Hennessy *et al.* (CLEO Collaboration), Phys. Rev. D **80**, 072001 (2009).
[12] M. Ablikim *et al.* (BESIII Collaboration), Chin. Phys. C **44**, 040001 (2020).
[13] M. Ablikim *et al.* (BESIII Collaboration), Nucl. Instrum. Methods Phys. Res., Sect. A **614**, 345 (2010).
[14] S. Agostinelli *et al.* (GEANT4 Collaboration), Nucl. Instrum. Methods Phys. Res., Sect. A **506**, 250 (2003).
[15] S. Jadach, B. F. L. Ward, and Z. Was, Comput. Phys. Commun. **130**, 260 (2000).
[16] S. Jadach, B. F. L. Ward, and Z. Was, Phys. Rev. D **63**, 113009 (2001).
[17] R. G. Ping, Chin. Phys. C **32**, 599 (2008).
[18] David J. Lange, Nucl. Instrum. Methods Phys. Res., Sect. A **462**, 152 (2001).
[19] P. U. E. Onyisi *et al.* (CLEO Collaboration), Phys. Rev. D **88**, 032009 (2013).
[20] M. Ablikim *et al.* (BESIII Collaboration), Phys. Rev. D **104**, 012016 (2021).
[21] E. Richter-Was, Phys. Lett. B **303**, 163 (1993).
[22] S. Navas *et al.* (Particle Data Group), Phys. Rev. D **110**, 030001 (2024).
[23] J. C. Chen, G. S. Huang, X. R. Qi, D. H. Zhang, and Y. S. Zhu, Phys. Rev. D **62**, 034003 (2000); R. L. Yang, R. G. Ping, and H. Chen, Chin. Phys. Lett. **31**, 061301 (2014).
[24] M. Ablikim *et al.* (BESIII Collaboration), Phys. Rev. D **101**, 112008 (2020).
[25] S. Actis *et al.*, Eur. Phys. J. C **66**, 585 (2010).
[26] Jerome H. Friedman, SMART User's Guide, Laboratory for Computational Statistics, Stanford University Technical Report No. 1, 1984, https://api.semanticscholar.org/CorpusID:60507696.
[27] Jerome H. Friedman, A variable span scatterplot smoother, Laboratory for Computational Statistics, Stanford University Technical Report No. 5, 1984, https://api.semanticscholar.org/CorpusID:222281453.
[28] W. Sun, T. Liu, M. Jing, L. Wang, B. Zhong, and W. Song, Front. Phys. (Beijing) **16**, 64501 (2021).
[29] See Supplemental Material at http://link.aps.org/supplemental/10.1103/PhysRevLett.133.261902 for detailed numbers of the cross sections, which include Refs. [30–34] for additional information about the center-of-mass energies and integrated luminosities and covariance systematic uncertainties matrix.
[30] M. Ablikim *et al.* (BESIII Collaboration), Chin. Phys. C **40**, 063001 (2016).
[31] M. Ablikim *et al.* (BESIII Collaboration), Chin. Phys. C **45**, 103001 (2021).
[32] M. Ablikim *et al.* (BESIII Collaboration), Chin. Phys. C **46**, 113003 (2022).
[33] M. Ablikim *et al.* (BESIII Collaboration), Chin. Phys. C **46**, 113002 (2022).
[34] M. Ablikim *et al.* (BESIII Collaboration), Chin. Phys. C **41**, 063001 (2017).
[35] E. Eichten, K. Gottfried, T. Kinoshita, K. D. Lane, and T. M. Yan, Phys. Rev. D **21**, 203 (1980).
[36] Xiang-Kun Dong, Liang-Liang Wang, and Chang-Zheng Yuan, Chin. Phys. C **42**, 043002 (2018).
[37] M. Ablikim *et al.* (BESIII Collaboration), Phys. Rev. Lett. **110**, 252001 (2013).
[38] Z. Q. Liu *et al.* (Belle Collaboration), Phys. Rev. Lett. **110**, 252002 (2013).
[39] E. van Beveren, G. Rupp, and M. D. Scadron, Phys. Lett. B **495**, 300 (2000).
[40] M. Ablikim *et al.* (BESIII Collaboration), Phys. Rev. D **97**, 071101 (2018).
[41] M. Ablikim *et al.* (BESIII Collaboration), Chin. Phys. C **39**, 093001 (2015).
[42] M. Ablikim *et al.* (BESIII Collaboration), Phys. Rev. D **91**, 032002 (2015).
[43] M. Ablikim *et al.* (BESIII Collaboration), Phys. Rev. Lett. **112**, 022001 (2014).
[44] L. C. Gui, L. S. Lu, Q. F. Lü, X. H. Zhong, and Q. Zhao, Phys. Rev. D **98**, 016010 (2018).
[45] T. V. Uglov, Y. S. Kalashnikova, A. V. Nefediev, G. V. Pakhlova, and P. N. Pakhlov, JETP Lett. **105**, 1 (2017).

M. Ablikim,[1] M. N. Achasov,[4,c] P. Adlarson,[75] O. Afedulidis,[3] X. C. Ai,[80] R. Aliberti,[35] A. Amoroso,[74a,74c] Q. An,[71,58,a] Y. Bai,[57] O. Bakina,[36] I. Balossino,[29a] Y. Ban,[46,h] H.-R. Bao,[63] V. Batozskaya,[1,44] K. Begzsuren,[32] N. Berger,[35] M. Berlowski,[44] M. Bertani,[28a] D. Bettoni,[29a] F. Bianchi,[74a,74c] E. Bianco,[74a,74c] A. Bortone,[74a,74c] I. Boyko,[36] R. A. Briere,[5] A. Brueggemann,[68] H. Cai,[76] X. Cai,[1,58] A. Calcaterra,[28a] G. F. Cao,[1,63] N. Cao,[1,63] S. A. Cetin,[62a] J. F. Chang,[1,58] G. R. Che,[43] G. Chelkov,[36,b] C. Chen,[43] C. H. Chen,[9] Chao Chen,[55] G. Chen,[1] H. S. Chen,[1,63] H. Y. Chen,[20] M. L. Chen,[1,58,63] S. J. Chen,[42] S. L. Chen,[45] S. M. Chen,[61] T. Chen,[1,63] X. R. Chen,[31,63] X. T. Chen,[1,63] Y. B. Chen,[1,58] Y. Q. Chen,[34] Z. J. Chen,[25,i] Z. Y. Chen,[1,63] S. K. Choi,[10] G. Cibinetto,[29a] F. Cossio,[74c] J. J. Cui,[50] H. L. Dai,[1,58] J. P. Dai,[78] A. Dbeyssi,[18] R. E. de Boer,[3] D. Dedovich,[36] C. Q. Deng,[72] Z. Y. Deng,[1] A. Denig,[35] I. Denysenko,[36] M. Destefanis,[74a,74c] F. De Mori,[74a,74c] B. Ding,[66,1] X. X. Ding,[46,h] Y. Ding,[40] Y. Ding,[34] J. Dong,[1,58] L. Y. Dong,[1,63] M. Y. Dong,[1,58,63] X. Dong,[76] M. C. Du,[1] S. X. Du,[80] Y. Y. Duan,[55] Z. H. Duan,[42] P. Egorov,[36,b] Y. H. Fan,[45] J. Fang,[59] J. Fang,[1,58] S. S. Fang,[1,63] W. X. Fang,[1] Y. Fang,[1] Y. Q. Fang,[1,58] R. Farinelli,[29a] L. Fava,[74b,74c] F. Feldbauer,[3] G. Felici,[28a] C. Q. Feng,[71,58] J. H. Feng,[59] Y. T. Feng,[71,58] M. Fritsch,[3] C. D. Fu,[1] J. L. Fu,[63] Y. W. Fu,[1,63] H. Gao,[63] X. B. Gao,[41] Y. N. Gao,[46,h] Yang Gao,[71,58] S. Garbolino,[74c] I. Garzia,[29a,29b] L. Ge,[80] P. T. Ge,[76] Z. W. Ge,[42] C. Geng,[59] E. M. Gersabeck,[67] A. Gilman,[69] K. Goetzen,[13]

L. Gong,[40] W. X. Gong,[1,58] W. Gradl,[35] S. Gramigna,[29a,29b] M. Greco,[74a,74c] M. H. Gu,[1,58] Y. T. Gu,[15] C. Y. Guan,[1,63] A. Q. Guo,[31,63] L. B. Guo,[41] M. J. Guo,[50] R. P. Guo,[49] Y. P. Guo,[12,g] A. Guskov,[36,b] J. Gutierrez,[27] K. L. Han,[63] T. T. Han,[1] F. Hanisch,[3] X. Q. Hao,[19] F. A. Harris,[65] K. K. He,[55] K. L. He,[1,63] F. H. Heinsius,[3] C. H. Heinz,[35] Y. K. Heng,[1,58,63] C. Herold,[60] T. Holtmann,[3] P. C. Hong,[34] G. Y. Hou,[1,63] X. T. Hou,[1,63] Y. R. Hou,[63] Z. L. Hou,[1] B. Y. Hu,[59] H. M. Hu,[1,63] J. F. Hu,[56,j] S. L. Hu,[12,g] T. Hu,[1,58,63] Y. Hu,[1] G. S. Huang,[71,58] K. X. Huang,[59] L. Q. Huang,[31,63] X. T. Huang,[50] Y. P. Huang,[1] Y. S. Huang,[59] T. Hussain,[73] F. Hölzken,[3] N. Hüsken,[35] N. in der Wiesche,[68] J. Jackson,[27] S. Janchiv,[32] J. H. Jeong,[10] Q. Ji,[1] Q. P. Ji,[19] W. Ji,[1,63] X. B. Ji,[1,63] X. L. Ji,[1,58] Y. Y. Ji,[50] X. Q. Jia,[50] Z. K. Jia,[71,58] D. Jiang,[1,63] H. B. Jiang,[76] P. C. Jiang,[46,h] S. S. Jiang,[39] T. J. Jiang,[16] X. S. Jiang,[1,58,63] Y. Jiang,[63] J. B. Jiao,[50] J. K. Jiao,[34] Z. Jiao,[23] S. Jin,[42] Y. Jin,[66] M. Q. Jing,[1,63] X. M. Jing,[63] T. Johansson,[75] S. Kabana,[33] N. Kalantar-Nayestanaki,[64] X. L. Kang,[9] X. S. Kang,[40] M. Kavatsyuk,[64] B. C. Ke,[80] V. Khachatryan,[27] A. Khoukaz,[68] R. Kiuchi,[1] O. B. Kolcu,[62a] B. Kopf,[3] M. Kuessner,[3] X. Kui,[1,63] N. Kumar,[26] A. Kupsc,[44,75] W. Kühn,[37] J. J. Lane,[67] P. Larin,[18] L. Lavezzi,[74a,74c] T. T. Lei,[71,58] Z. H. Lei,[71,58] M. Lellmann,[35] T. Lenz,[35] C. Li,[43] C. Li,[47] C. H. Li,[39] Cheng Li,[71,58] D. M. Li,[80] F. Li,[1,58] G. Li,[1] H. B. Li,[1,63] H. J. Li,[19] H. N. Li,[56,j] Hui Li,[43] J. R. Li,[61] J. S. Li,[59] K. Li,[1] L. J. Li,[1,63] L. K. Li,[1] Lei Li,[48] M. H. Li,[43] P. R. Li,[38,k,l] Q. M. Li,[1,63] Q. X. Li,[50] R. Li,[17,31] S. X. Li,[12] T. Li,[50] W. D. Li,[1,63] W. G. Li,[1,a] X. Li,[1,63] X. H. Li,[71,58] X. L. Li,[50] X. Y. Li,[1,63] X. Z. Li,[59] Y. G. Li,[46,h] Z. J. Li,[59] Z. Y. Li,[78] C. Liang,[42] H. Liang,[1,63] H. Liang,[71,58] Y. F. Liang,[54] Y. T. Liang,[31,63] G. R. Liao,[14] L. Z. Liao,[50] Y. P. Liao,[1,63] J. Libby,[26] A. Limphirat,[60] C. C. Lin,[55] D. X. Lin,[31,63] T. Lin,[1] B. J. Liu,[1] B. X. Liu,[76] C. Liu,[34] C. X. Liu,[1] F. Liu,[1] F. H. Liu,[53] Feng Liu,[6] G. M. Liu,[56,j] H. Liu,[38,k,l] H. B. Liu,[15] H. H. Liu,[1] H. M. Liu,[1,63] Huihui Liu,[21] J. B. Liu,[71,58] J. Y. Liu,[1,63] K. Liu,[38,k,l] K. Y. Liu,[40] Ke Liu,[22] L. Liu,[71,58] L. C. Liu,[43] Lu Liu,[43] M. H. Liu,[12,g] P. L. Liu,[1] Q. Liu,[63] S. B. Liu,[71,58] T. Liu,[12,g] W. K. Liu,[43] W. M. Liu,[71,58] X. Liu,[38,k,l] X. Liu,[39] Y. Liu,[80] Y. Liu,[38,k,l] Y. B. Liu,[43] Z. A. Liu,[1,58,63] Z. D. Liu,[9] Z. Q. Liu,[50] X. C. Lou,[1,58,63] F. X. Lu,[59] H. J. Lu,[23] J. G. Lu,[1,58] X. L. Lu,[1] Y. Lu,[7] Y. P. Lu,[1,58] Z. H. Lu,[1,63] C. L. Luo,[41] J. R. Luo,[59] M. X. Luo,[79] T. Luo,[12,g] X. L. Luo,[1,58] X. R. Lyu,[63] Y. F. Lyu,[43] F. C. Ma,[40] H. Ma,[78] H. L. Ma,[1] J. L. Ma,[1,63] L. L. Ma,[50] M. M. Ma,[1,63] Q. M. Ma,[1] R. Q. Ma,[1,63] T. Ma,[71,58] X. T. Ma,[1,63] X. Y. Ma,[1,58] Y. Ma,[46,h] Y. M. Ma,[31] F. E. Maas,[18] M. Maggiora,[74a,74c] S. Malde,[69] Y. J. Mao,[46,h] Z. P. Mao,[1] S. Marcello,[74a,74c] Z. X. Meng,[66] J. G. Messchendorp,[13,64] G. Mezzadri,[29a] H. Miao,[1,63] T. J. Min,[42] R. E. Mitchell,[27] X. H. Mo,[1,58,63] B. Moses,[27] N. Yu. Muchnoi,[4,c] J. Muskalla,[35] Y. Nefedov,[36] F. Nerling,[18,e] L. S. Nie,[20] I. B. Nikolaev,[4,c] Z. Ning,[1,58] S. Nisar,[11,m] Q. L. Niu,[38,k,l] W. D. Niu,[55] Y. Niu,[50] S. L. Olsen,[63] Q. Ouyang,[1,58,63] S. Pacetti,[28b,28c] X. Pan,[55] Y. Pan,[57] A. Pathak,[34] P. Patteri,[28a] Y. P. Pei,[71,58] M. Pelizaeus,[3] H. P. Peng,[71,58] Y. Y. Peng,[38,k,l] K. Peters,[13,e] J. L. Ping,[41] R. G. Ping,[1,63] S. Plura,[35] V. Prasad,[33] F. Z. Qi,[1] H. Qi,[71,58] H. R. Qi,[61] M. Qi,[42] T. Y. Qi,[12,g] S. Qian,[1,58] W. B. Qian,[63] C. F. Qiao,[63] X. K. Qiao,[80] J. J. Qin,[72] L. Q. Qin,[14] L. Y. Qin,[71,58] X. S. Qin,[50] Z. H. Qin,[1,58] J. F. Qiu,[1] Z. H. Qu,[72] C. F. Redmer,[35] K. J. Ren,[39] A. Rivetti,[74c] M. Rolo,[74c] G. Rong,[1,63] Ch. Rosner,[18] S. N. Ruan,[43] N. Salone,[44] A. Sarantsev,[36,d] Y. Schelhaas,[35] K. Schoenning,[75] M. Scodeggio,[29a] K. Y. Shan,[12,g] W. Shan,[24] X. Y. Shan,[71,58] Z. J. Shang,[38,k,l] J. F. Shangguan,[16] L. G. Shao,[1,63] M. Shao,[71,58] C. P. Shen,[12,g] H. F. Shen,[1,8] W. H. Shen,[63] X. Y. Shen,[1,63] B. A. Shi,[63] H. Shi,[71,58] H. C. Shi,[71,58] J. L. Shi,[12,g] J. Y. Shi,[1] Q. Q. Shi,[55] S. Y. Shi,[72] X. Shi,[1,58] J. J. Song,[19] T. Z. Song,[59] W. M. Song,[34,1] Y. J. Song,[12,g] Y. X. Song,[46,h,n] S. Sosio,[74a,74c] S. Spataro,[74a,74c] F. Stieler,[35] Y. J. Su,[63] G. B. Sun,[76] G. X. Sun,[1] H. Sun,[63] H. K. Sun,[1] J. F. Sun,[19] K. Sun,[61] L. Sun,[76] S. S. Sun,[1,63] T. Sun,[51,f] W. Y. Sun,[34] Y. Sun,[9] Y. J. Sun,[71,58] Y. Z. Sun,[1] Z. Q. Sun,[1,63] Z. T. Sun,[50] C. J. Tang,[54] G. Y. Tang,[1] J. Tang,[59] M. Tang,[71,58] Y. A. Tang,[76] L. Y. Tao,[72] Q. T. Tao,[25,i] M. Tat,[69] J. X. Teng,[71,58] V. Thoren,[75] W. H. Tian,[59] Y. Tian,[31,63] Z. F. Tian,[76] I. Uman,[62b] Y. Wan,[55] S. J. Wang,[50] B. Wang,[1] B. L. Wang,[63] Bo Wang,[71,58] D. Y. Wang,[46,h] F. Wang,[72] H. J. Wang,[38,k,l] J. J. Wang,[76] J. P. Wang,[50] K. Wang,[1,58] L. L. Wang,[1] M. Wang,[50] N. Y. Wang,[63] S. Wang,[12,g] S. Wang,[38,k,l] T. Wang,[12,g] T. J. Wang,[43] W. Wang,[72] W. Wang,[59] W. P. Wang,[35,71,o] X. Wang,[46,h] X. F. Wang,[38,k,l] X. J. Wang,[39] X. L. Wang,[12,g] X. N. Wang,[1] Y. Wang,[61] Y. D. Wang,[45] Y. F. Wang,[1,58,63] Y. L. Wang,[19] Y. N. Wang,[45] Y. Q. Wang,[1] Yaqian Wang,[17] Yi Wang,[61] Z. Wang,[1,58] Z. L. Wang,[72] Z. Y. Wang,[1,63] Ziyi Wang,[63] D. H. Wei,[14] F. Weidner,[68] S. P. Wen,[1] Y. R. Wen,[39] U. Wiedner,[3] G. Wilkinson,[69] M. Wolke,[75] L. Wollenberg,[3] C. Wu,[39] J. F. Wu,[1,8] L. H. Wu,[1] L. J. Wu,[1,63] X. Wu,[12,g] X. H. Wu,[34] Y. Wu,[71,58] Y. H. Wu,[55] Y. J. Wu,[31] Z. Wu,[1,58] L. Xia,[71,58] X. M. Xian,[39] B. H. Xiang,[1,63] T. Xiang,[46,h] D. Xiao,[38,k,l] G. Y. Xiao,[42] S. Y. Xiao,[1] Y. L. Xiao,[12,g] Z. J. Xiao,[41] C. Xie,[42] X. H. Xie,[46,h] Y. Xie,[50] Y. G. Xie,[1,58] Y. H. Xie,[6] Z. P. Xie,[71,58] T. Y. Xing,[1,63] C. F. Xu,[1,63] C. J. Xu,[59] G. F. Xu,[1] H. Y. Xu,[66,2,p] M. Xu,[71,58] Q. J. Xu,[16] Q. N. Xu,[30] W. Xu,[1] W. L. Xu,[66] X. P. Xu,[55] Y. C. Xu,[77] Z. P. Xu,[42] Z. S. Xu,[63] F. Yan,[12,g] L. Yan,[12,g] W. B. Yan,[71,58] W. C. Yan,[80] X. Q. Yan,[1] H. J. Yang,[51,f] H. L. Yang,[34] H. X. Yang,[1] T. Yang,[1] Y. Yang,[12,g] Y. F. Yang,[43] Y. F. Yang,[1,63] Y. X. Yang,[1,63] Z. W. Yang,[38,k,l] Z. P. Yao,[50] M. Ye,[1,58] M. H. Ye,[8] J. H. Yin,[1] Z. Y. You,[59] B. X. Yu,[1,58,63] C. X. Yu,[43] G. Yu,[1,63] J. S. Yu,[25,i] T. Yu,[72] X. D. Yu,[46,h] Y. C. Yu,[80] C. Z. Yuan,[1,63]

J. Yuan,[45] J. Yuan,[34] L. Yuan,[2] S. C. Yuan,[1,63] Y. Yuan,[1,63] Z. Y. Yuan,[59] C. X. Yue,[39] A. A. Zafar,[73] F. R. Zeng,[50] S. H. Zeng,[72] X. Zeng,[12,g] Y. Zeng,[25,i] Y. J. Zeng,[1,63] Y. J. Zeng,[59] X. Y. Zhai,[34] Y. C. Zhai,[50] Y. H. Zhan,[59] A. Q. Zhang,[1,63] B. L. Zhang,[1,63] B. X. Zhang,[1] D. H. Zhang,[43] G. Y. Zhang,[19] H. Zhang,[80] H. Zhang,[71,58] H. C. Zhang,[1,58,63] H. H. Zhang,[59] H. H. Zhang,[34] H. Q. Zhang,[1,58,63] H. R. Zhang,[71,58] H. Y. Zhang,[1,58] J. Zhang,[80] J. Zhang,[59] J. J. Zhang,[52] J. L. Zhang,[20] J. Q. Zhang,[41] J. S. Zhang,[12,g] J. W. Zhang,[1,58,63] J. X. Zhang,[38,k,l] J. Y. Zhang,[1] J. Z. Zhang,[1,63] Jianyu Zhang,[63] L. M. Zhang,[61] Lei Zhang,[42] P. Zhang,[1,63] Q. Y. Zhang,[34] R. Y. Zhang,[38,k,l] S. H. Zhang,[1,63] Shulei Zhang,[25,i] X. D. Zhang,[45] X. M. Zhang,[1] X. Y. Zhang,[50] Y. Zhang,[72] Y. Zhang,[1] Y. T. Zhang,[80] Y. H. Zhang,[1,58] Y. M. Zhang,[39] Yan Zhang,[71,58] Z. D. Zhang,[1] Z. H. Zhang,[1] Z. L. Zhang,[34] Z. Y. Zhang,[43] Z. Y. Zhang,[76] Z. Z. Zhang,[45] G. Zhao,[1] J. Y. Zhao,[1,63] J. Z. Zhao,[1,58] L. Zhao,[1] Lei Zhao,[71,58] M. G. Zhao,[43] N. Zhao,[78] R. P. Zhao,[63] S. J. Zhao,[80] Y. B. Zhao,[1,58] Y. X. Zhao,[31,63] Z. G. Zhao,[71,58] A. Zhemchugov,[36,b] B. Zheng,[72] B. M. Zheng,[34] J. P. Zheng,[1,58] W. J. Zheng,[1,63] Y. H. Zheng,[63] B. Zhong,[41] X. Zhong,[59] H. Zhou,[50] J. Y. Zhou,[34] L. P. Zhou,[1,63] S. Zhou,[6] X. Zhou,[76] X. K. Zhou,[6] X. R. Zhou,[71,58] X. Y. Zhou,[39] Y. Z. Zhou,[12,g] J. Zhu,[43] K. Zhu,[1] K. J. Zhu,[1,58,63] K. S. Zhu,[12,g] L. Zhu,[34] L. X. Zhu,[63] S. H. Zhu,[70] S. Q. Zhu,[42] T. J. Zhu,[12,g] W. D. Zhu,[41] Y. C. Zhu,[71,58] Z. A. Zhu,[1,63] J. H. Zou,[1] and J. Zu[71,58]

(BESIII Collaboration)

[1]*Institute of High Energy Physics, Beijing 100049, People's Republic of China*
[2]*Beihang University, Beijing 100191, People's Republic of China*
[3]*Bochum Ruhr-University, D-44780 Bochum, Germany*
[4]*Budker Institute of Nuclear Physics SB RAS (BINP), Novosibirsk 630090, Russia*
[5]*Carnegie Mellon University, Pittsburgh, Pennsylvania 15213, USA*
[6]*Central China Normal University, Wuhan 430079, People's Republic of China*
[7]*Central South University, Changsha 410083, People's Republic of China*
[8]*China Center of Advanced Science and Technology, Beijing 100190, People's Republic of China*
[9]*China University of Geosciences, Wuhan 430074, People's Republic of China*
[10]*Chung-Ang University, Seoul, 06974, Republic of Korea*
[11]*COMSATS University Islamabad, Lahore Campus, Defence Road, Off Raiwind Road, 54000 Lahore, Pakistan*
[12]*Fudan University, Shanghai 200433, People's Republic of China*
[13]*GSI Helmholtzcentre for Heavy Ion Research GmbH, D-64291 Darmstadt, Germany*
[14]*Guangxi Normal University, Guilin 541004, People's Republic of China*
[15]*Guangxi University, Nanning 530004, People's Republic of China*
[16]*Hangzhou Normal University, Hangzhou 310036, People's Republic of China*
[17]*Hebei University, Baoding 071002, People's Republic of China*
[18]*Helmholtz Institute Mainz, Staudinger Weg 18, D-55099 Mainz, Germany*
[19]*Henan Normal University, Xinxiang 453007, People's Republic of China*
[20]*Henan University, Kaifeng 475004, People's Republic of China*
[21]*Henan University of Science and Technology, Luoyang 471003, People's Republic of China*
[22]*Henan University of Technology, Zhengzhou 450001, People's Republic of China*
[23]*Huangshan College, Huangshan 245000, People's Republic of China*
[24]*Hunan Normal University, Changsha 410081, People's Republic of China*
[25]*Hunan University, Changsha 410082, People's Republic of China*
[26]*Indian Institute of Technology Madras, Chennai 600036, India*
[27]*Indiana University, Bloomington, Indiana 47405, USA*
[28a]*INFN Laboratori Nazionali di Frascati, INFN Laboratori Nazionali di Frascati, I-00044, Frascati, Italy*
[28b]*INFN Sezione di Perugia, I-06100, Perugia, Italy*
[28c]*University of Perugia, I-06100, Perugia, Italy*
[29a]*INFN Sezione di Ferrara, INFN Sezione di Ferrara, I-44122, Ferrara, Italy*
[29b]*University of Ferrara, I-44122, Ferrara, Italy*
[30]*Inner Mongolia University, Hohhot 010021, People's Republic of China*
[31]*Institute of Modern Physics, Lanzhou 730000, People's Republic of China*
[32]*Institute of Physics and Technology, Peace Avenue 54B, Ulaanbaatar 13330, Mongolia*
[33]*Instituto de Alta Investigación, Universidad de Tarapacá, Casilla 7D, Arica 1000000, Chile*
[34]*Jilin University, Changchun 130012, People's Republic of China*
[35]*Johannes Gutenberg University of Mainz, Johann-Joachim-Becher-Weg 45, D-55099 Mainz, Germany*
[36]*Joint Institute for Nuclear Research, 141980 Dubna, Moscow region, Russia*
[37]*Justus-Liebig-Universitaet Giessen, II, Physikalisches Institut, Heinrich-Buff-Ring 16, D-35392 Giessen, Germany*

[38]Lanzhou University, Lanzhou 730000, People's Republic of China
[39]Liaoning Normal University, Dalian 116029, People's Republic of China
[40]Liaoning University, Shenyang 110036, People's Republic of China
[41]Nanjing Normal University, Nanjing 210023, People's Republic of China
[42]Nanjing University, Nanjing 210093, People's Republic of China
[43]Nankai University, Tianjin 300071, People's Republic of China
[44]National Centre for Nuclear Research, Warsaw 02-093, Poland
[45]North China Electric Power University, Beijing 102206, People's Republic of China
[46]Peking University, Beijing 100871, People's Republic of China
[47]Qufu Normal University, Qufu 273165, People's Republic of China
[48]Renmin University of China, Beijing 100872, People's Republic of China
[49]Shandong Normal University, Jinan 250014, People's Republic of China
[50]Shandong University, Jinan 250100, People's Republic of China
[51]Shanghai Jiao Tong University, Shanghai 200240, People's Republic of China
[52]Shanxi Normal University, Linfen 041004, People's Republic of China
[53]Shanxi University, Taiyuan 030006, People's Republic of China
[54]Sichuan University, Chengdu 610064, People's Republic of China
[55]Soochow University, Suzhou 215006, People's Republic of China
[56]South China Normal University, Guangzhou 510006, People's Republic of China
[57]Southeast University, Nanjing 211100, People's Republic of China
[58]State Key Laboratory of Particle Detection and Electronics, Beijing 100049, Hefei 230026, People's Republic of China
[59]Sun Yat-Sen University, Guangzhou 510275, People's Republic of China
[60]Suranaree University of Technology, University Avenue 111, Nakhon Ratchasima 30000, Thailand
[61]Tsinghua University, Beijing 100084, People's Republic of China
[62a]Turkish Accelerator Center Particle Factory Group, Istinye University, 34010 Istanbul, Turkey
[62b]Near East University, Nicosia, North Cyprus, 99138, Mersin 10, Turkey
[63]University of Chinese Academy of Sciences, Beijing 100049, People's Republic of China
[64]University of Groningen, NL-9747 AA Groningen, The Netherlands
[65]University of Hawaii, Honolulu, Hawaii 96822, USA
[66]University of Jinan, Jinan 250022, People's Republic of China
[67]University of Manchester, Oxford Road, Manchester, M13 9PL, United Kingdom
[68]University of Muenster, Wilhelm-Klemm-Strasse 9, 48149 Muenster, Germany
[69]University of Oxford, Keble Road, Oxford OX13RH, United Kingdom
[70]University of Science and Technology Liaoning, Anshan 114051, People's Republic of China
[71]University of Science and Technology of China, Hefei 230026, People's Republic of China
[72]University of South China, Hengyang 421001, People's Republic of China
[73]University of the Punjab, Lahore-54590, Pakistan
[74a]University of Turin and INFN, University of Turin, I-10125, Turin, Italy
[74b]University of Eastern Piedmont, I-15121, Alessandria, Italy
[74c]INFN, I-10125, Turin, Italy
[75]Uppsala University, Box 516, SE-75120 Uppsala, Sweden
[76]Wuhan University, Wuhan 430072, People's Republic of China
[77]Yantai University, Yantai 264005, People's Republic of China
[78]Yunnan University, Kunming 650500, People's Republic of China
[79]Zhejiang University, Hangzhou 310027, People's Republic of China
[80]Zhengzhou University, Zhengzhou 450001, People's Republic of China

[a]Deceased.
[b]Also at the Moscow Institute of Physics and Technology, Moscow 141700, Russia.
[c]Also at the Novosibirsk State University, Novosibirsk, 630090, Russia.
[d]Also at the NRC "Kurchatov Institute", PNPI, 188300, Gatchina, Russia.
[e]Also at Goethe University Frankfurt, 60323 Frankfurt am Main, Germany.
[f]Also at Key Laboratory for Particle Physics, Astrophysics and Cosmology, Ministry of Education; Shanghai Key Laboratory for Particle Physics and Cosmology; Institute of Nuclear and Particle Physics, Shanghai 200240, People's Republic of China.
[g]Also at Key Laboratory of Nuclear Physics and Ion-beam Application (MOE) and Institute of Modern Physics, Fudan University, Shanghai 200443, People's Republic of China.
[h]Also at State Key Laboratory of Nuclear Physics and Technology, Peking University, Beijing 100871, People's Republic of China.
[i]Also at School of Physics and Electronics, Hunan University, Changsha 410082, People's Republic of China.
[j]Also at Guangdong Provincial Key Laboratory of Nuclear Science, Institute of Quantum Matter, South China Normal University, Guangzhou 510006, People's Republic of China.

[k]Also at MOE Frontiers Science Center for Rare Isotopes, Lanzhou University, Lanzhou 730000, People's Republic of China.
[l]Also at Lanzhou Center for Theoretical Physics, Lanzhou University, Lanzhou 730000, People's Republic of China.
[m]Also at the Department of Mathematical Sciences, IBA, Karachi 75270, Pakistan.
[n]Also at Ecole Polytechnique Federale de Lausanne (EPFL), CH-1015 Lausanne, Switzerland.
[o]Also at Helmholtz Institute Mainz, Staudinger Weg 18, D-55099 Mainz, Germany.
[p]Also at School of Physics, Beihang University, Beijing 100191, People's Republic of China.